Peripapillary and Macular Vessel Density in Dysthyroid Optic Neuropathy: An Optical Coherence Tomography Angiography Study

Te Zhang, Wei Xiao, Huijing Ye, Rongxin Chen, Yuxiang Mao, and Huasheng Yang

State Key Laboratory of Ophthalmology, Zhongshan Ophthalmic Center, Sun Yat-sen University, Guangzhou, China

Correspondence: Huasheng Yang, Zhongshan Ophthalmic Center, Guangzhou 510060, People's Republic of China; yanghuasheng@gzzoc.com.

TZ, WX, and HY contributed equally to the work presented here and should therefore be regarded as equivalent authors.

PURPOSE. To evaluate peripapillary and macular vessel density in eyes with dysthyroid optic neuropathy (DON) and its correlation with visual function.

METHODS. Patients diagnosed as thyroid-associated ophthalmopathy (TAO) with or without DON and healthy participants were recruited. All subjects underwent a complete ophthalmic examination and optical coherence tomography angiography centered on the fovea and the optic nerve head. Microvascular measurements were summarized as vessel density in the whole image and in each subfield. Visual function, including best-corrected visual acuity (BCVA), visual field (VF), and visual evoked potential (VEP), were assessed for all TAO patients. Areas under the receiver operating characteristic curves (AUROCs) were applied to evaluate the diagnostic accuracy of vessel density for DON.

RESULTS. A total of 23 healthy eyes, 41 TAO eyes without DON, and 30 with DON were studied. The radial peripapillary capillary whole image vessel density (rpc-wiVD) and optic nerve head whole image vessel density (onh-wiVD) were significantly decreased in DON eyes compared with healthy and non-DON eyes (all $P < 0.05$). The decrease was more profound in the temporal peripapillary subfields than in others. The impairment of visual function (i.e. BCVA, VF, and VEP) was positively associated with the reduction of onh-wiVD and rpc-wiVD but not related to the rarefaction of macular microvasculature. Moreover, the onh-wiVD showed desirable diagnostic capacity to distinguish the DON eyes from NDON eyes (AUROC, 0.75).

CONCLUSIONS. A decrease in vessel density in the peripapillary area is evident in eyes with DON. The attenuation in peripapillary perfusion significantly correlates to the extent of visual impairment.

Keywords: thyroid-associated ophthalmopathy, dysthyroid optic neuropathy, optical coherence tomography angiography, retinal vessel density

Thyroid-associated ophthalmopathy (TAO), also known as Graves' ophthalmopathy, is an autoimmune disorder that predominantly affects patients with Graves' hyperthyroidism.[1] It presents with a spectrum of clinical findings according to the ocular tissues affected, from eyelid retraction, proptosis to cornea exposure, and apical compression of the optic nerve.[2] The most frequent vision-threatening condition of TAO is dysthyroid optic neuropathy (DON), which involves 4% to 8% of all TAO patients.[3] The exact pathogenesis of DON remains unclear but might be related to the mechanical compression from the enlarged extraocular muscles and excessive soft tissue.[4] The compression may directly stretch the optic nerve on one hand and reduce the blood flow in short posterior ciliary and peripapillary retinal arteries on the other.[5,6] A report showed that superior ophthalmic vein blood flow velocity was significantly decreased in DON eyes, which implies that the abnormal hemodynamic state may participate in the development of DON.[7]

Optical coherence tomography angiography (OCT-A) is a noninvasive technique capable of qualitatively and quantitatively evaluating the retinal and choroidal perfusion.[8,9] It has been recently introduced to assess the retinal vasculature in glaucoma,[10-13] diabetic retinopathy,[14] age-related macular degeneration,[15] and several optic neuropathies,[16-18] and helped in diagnosing these diseases.[19] The mechanism underlying DON appears to be multifactorial, and vascular insufficiency might be an important factor as in other optic neuropathies.[5,6] With the emergence of OCT-A, it is feasible to figure out the correlation between microvascular perfusion and the development of DON. A recent OCT-A study investigating the retinal vessel changes in active TAO eyes initiated the exploration to the contribution of intraocular blood flow in the development of TAO.[20] In this study, however, we focused primarily on the patients with severe TAO (i.e., those complicated with DON), and also aimed to elucidate the relation of microvascular perfusion and visual function impairment.

METHODS

Study Population

TAO patients with or without DON were recruited from Zhongshan Ophthalmic Center from April 1, 2018 to July 1,

2018. Age- and sex-matched healthy subjects were enrolled simultaneously. Written informed consent was obtained prior to any examination. This study was conducted adhering to the tenets of the Declaration of Helsinki.

The diagnosis of TAO and severity classification were made using the European Group on Graves' Orbitopathy criteria.[21] The TAO patients meeting the following criteria were included in the study: (1) age of >18 years, (2) spherical equivalent of <3.00 diopters (D), (3) clear refractive media allowing sufficient image quality, and (4) no treatment with systemic glucocorticoids for at least 3 months prior to the study. The common exclusion criteria for all subjects were as follows: (1) any systemic diseases rather than thyroid disorders, (2) any history of ocular surgery or ocular trauma, and (3) any ophthalmopathies (e.g., glaucoma, diabetic retinopathy, and uveitis). DON was diagnosed based on clinical findings[6,22,23]: decreased visual acuity (the best-corrected visual acuity [BCVA] in logMAR visual chart, >0.2), apparent visual field (VF) defect (mean deviation [MD] in Humphrey perimetry, <−10 dB), relative afferent pupillary defect when unilaterally affected, abnormal pattern visual evoked potentials test (latency delay and amplitude reduction), and evident apical crowding in orbital computed tomography or and/or magnetic resonance imaging. As image quality was associated with the vessel density measures,[24] OCT-A scans with inadequate quality were excluded: (1) signal strength index of <45, (2) motion artifacts visible on the en face angiogram, (3) local weak signal, and (4) images off-center on fovea or disc.

Ophthalmic and Systemic Examination

All subjects underwent a comprehensive ocular examination, including BCVA, refraction, axial length measurement, Goldmann applanation tonometry, slit-lamp biomicroscopy, fundoscopy, apparent pupillary defect evaluation, and ocular motility assessment. The severity and the clinical activity of thyroid eye disease were graded according to the NOSPECS classification (N = no symptoms or signs, O = only signs, S = soft tissue involvement, P = proptosis, E = extraocular muscle involvement, C = corneal involvement, S = sight loss due to optic nerve compression) and the seven-item clinical activity score scheme,[21,25] respectively. Ancillary tests, including orbital computed tomography (Mx8000 IDT; Philips, Amsterdam, The Netherlands) and/or magnetic resonance imaging (Achieva 1.5 T; Philips), Humphrey VF (Humphrey Field Analyzer II 750; Carl Zeiss Meditec, Inc., Dublin, CA, USA), pattern visual evoked potential (ESPION; Diagnosys LLC, Inc., Cambridge, UK) were only performed for all TAO subjects. Blood pressure was measured after at least 5 minutes of resting. Mean arterial blood pressure was computed as diastolic blood pressure plus one-third of pulse pressure.

Optical Coherence Tomography Angiography

All subjects were examined under a single OCT-A system (AngioVue; Optovue, Inc., Fremont, CA, USA), which was able to visualize and quantify the microvasculature at different retinal layers. The scanning speed of the device was 70,000 A-scans per second, and the central wavelength was 840 nm. Motion artifacts are minimized with the eye tracking system. Each studied eye underwent a 4.5 × 4.5-mm cube angio scan centered on the optic nerve head (ONH), and a 3.0 × 3.0-mm macular cube angio scan centered on the fovea. A split-spectrum amplitude decorrelation angiography algorithm was applied to produce OCT-A images.[26]

Vessel density was defined as the percentage of perfused vascular area in relation to the whole selected region in en face views. All vessel density parameters were automatically calculated using the built-in program. Peripapillary vessel density parameters, including the ONH whole image vessel density (onh-wiVD) and the radial peripapillary capillary whole image vessel density (rpc-wiVD), were generated from the 4.5 × 4.5-mm cube angio scan centered on the ONH. The macular whole image vessel density (m-wiVD) was obtained from the 3.0 × 3.0-mm cube angio scan centered on the fovea. The macular scanning area was segmented by an annular grid into 6 fields: temporal, superior, nasal, inferior, fovea, and parafoveal zones (Fig. 1A, 1C, 1E). The ONH scanning area was further divided into 8 sessions by an ONH grid (Fig. 1B, 1D, 1F): temporal, nasal, inferonasal, inferotemporal, supratemporal, supranasal, the inside-disc, and peripapillary fields.

Apart from vessel density indices, the OCT platform also segmented the retinal nerve fiber layer (RNFL) from the ONH B-scan and the retinal ganglion cell complex layer (GCCL) from the macular B-scan. Thicknesses of RNFL and GCCL were automatedly measured.

Statistical Analysis

Continuous variables were described as means ± standard deviation (SD). Differences of OCT-A measures (e.g., m-wiVD, onh-wiVD, and rpc-wiVD) across groups were tested with ANOVA. Bonferroni correction was applied to post hoc multiple comparisons between groups. The correlation between visual function (BCVA, VF-MD, VF-pattern standard deviation [VF-PSD], P100 latency, and P100 amplitude) and the microvascular density parameters was tested with Pearson's correlation analysis. Statistical analysis was performed using statistical software (SPSS version 20; IBM Corp., Armonk, NY, USA). A *P* value of <0.05 was considered to be statistically significant.

RESULTS

A total of 65 participants was enrolled in this study, with 19 (29.2%) healthy control (HC group), 27 (41.6%) TAO patients without DON (NDON group), and 19 (29.2%) TAO patients with DON (DON group). There was no difference in sex distribution (*P* = 0.769), age (*P* = 0.440), systolic blood pressure (*P* = 0.917), diastolic blood pressure (*P* = 0.847), and mean arterial blood pressure (*P* = 0.643) among the three groups (Table 1).

There were 23 healthy (24.5%), 41 NDON (43.6%), and 30 DON (31.9%) eyes included in the analysis. In terms of the clinical characteristics, there were no significant differences in the mean axial length and spherical equivalent (Table 2; *P* = 0.101 and 0.245, respectively). Compared to the healthy eyes, however, the TAO eyes (either with or without DON) had a worse mean BCVA and slightly higher intraocular pressure (Table 2; *P* < 0.001 and *P* = 0.002, respectively). All visual function parameters, including BCVA, VF-MD, VF-PSD, P100 latency, and P100 amplitude, were significantly different between the NDON and DON groups (Table 2; *P* < 0.05 for all).

Macular Vessel Density Parameters

The macular vessel density parameters across study groups were listed in Table 3. In 1-way ANOVA analysis, statistically significant differences were found among the groups for all macular vessel density measurements (all *P* < 0.05). In the post hoc pairwise analysis, the vessel density in the whole macular image (m-wiVD) and in all grid sessions except fovea in NDON eyes was significantly lower than those in healthy eyes (Table 3). Nevertheless, there was no significant difference in any macular vessel density indices between DON and NDON eyes (all *P* > 0.05).
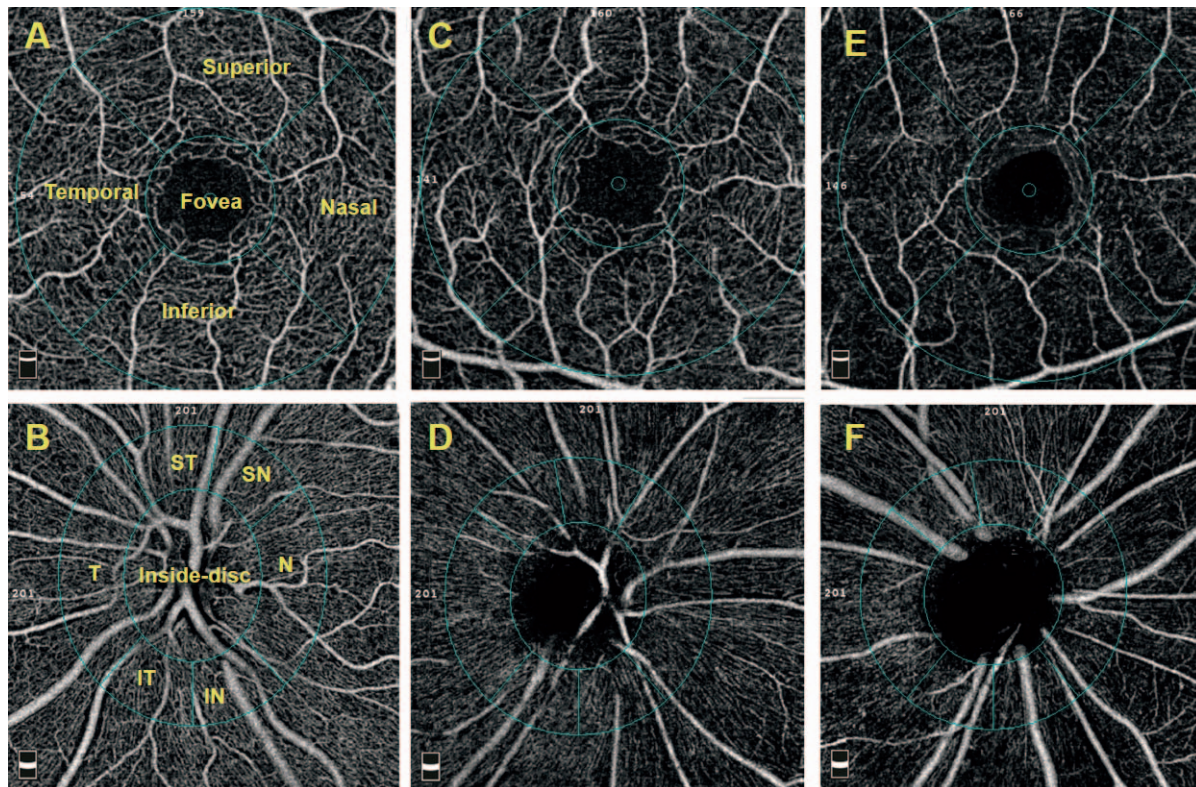
FIGURE 1. Representative OCT-A images in different groups. Macular vessel density map in healthy eye (**A**), NDON (**C**), and DON (**E**) eyes. Peripapillary vessel density map in healthy eye (**B**), NDON (**D**), and DON (**F**) eyes.

Peripapillary Vessel Density Parameters

The ONH and radial peripapillary capillary (RPC) vessel parameters across groups were listed in Table 4 and Table 5, respectively. Similar to the tendencies in the macular vessel density, the difference of vessel density in ONH whole image (onh-wiVD) and in each grid session were statistically significant among groups (all $P < 0.05$). Through multiple pairwise comparisons with Bonferroni correction, the DON eyes had the lowest onh-wiVD, and vessel densities in the peripapillary and temporal sessions (i.e. temporal, inferotemporal, and supratemporal) (Table 4; all $P < 0.05$). Compared to the healthy controls, the NDON eyes had significantly lower vessel densities in the whole ONH image ($P = 0.006$), in the inside-disc session ($P = 0.030$), and temporal session ($P = 0.003$) (Table 4). The differences in the rpc-wiVD and vessel densities in each grid session were statistically significant across groups (Table 5; all $P < 0.05$). Post hoc analysis demonstrated highly similar patterns as those of ONH vessel densities.

RNFL and GCCL Thicknesses

The thicknesses of RNFL and GCCL were listed in Table 6. The overall differences in RNFL and GCCL thicknesses among the three groups were significant ($P = 0.040$ and 0.008, respectively). Compared with NDON eyes, DON eyes had thinner mean GCCL thickness (post hoc $P = 0.026$), whereas the RNFL thickness was comparable (post hoc $P = 0.511$).

Correlation Between Vessel Density and Visual Function Parameters

We analyzed the correlation of macular and peripapillary vessel density with visual function parameters, including BCVA, VF-MD, VF-PSD, and visual evoked potential P100 latency and amplitude. Pearson correlation coefficients and their corresponding P values were listed in Table 7. The m-wiVD was only positively associated with P100 amplitude ($\gamma = 0.246$, $P = 0.039$) but not statistically associated with any other visual function parameters. Nevertheless, the onh-wiVD and rpc-wiVD were positively correlated with VF-MD and P100 amplitude (all $P < 0.001$) and negatively correlated with BCVA, VF PSD, and visual evoked potential P100 latency (all $P < 0.05$).

Diagnostic Abilities of Vessel Density Indices

The areas under the receiver operating characteristic curves (AUROCs) for distinguishing DON eyes from NDON eyes were highest for onh-wiVD (0.75), followed by rpc-wiVD (0.65), m-wiVD (0.61), GCCL (0.61), and RNFL (0.55) (Fig. 2). In the pairwise comparison, the onh-wiVD had a significantly higher AUROC than others in differentiating DON from NDON eyes.

TABLE 1. Demographic Characteristics of All Enrolled Subjects

Variables	HC	NDON	DON	*P*
N	19	27	19	NA
Sex, male, *n* (%)	10 (52.6)	13 (48.1)	8 (42.1)	0.769*
Age, y	46.7 ± 13.0	46.6 ± 9.2	53.9 ± 9.1	0.440
SBP, mm Hg	123.3 ± 9.8	123.2 ± 9.5	124.4 ± 11.7	0.917
DBP, mm Hg	77.5 ± 7.3	77.8 ± 8.2	76.5 ± 6.3	0.847
MABP, mm Hg	92.8 ± 7.3	93.8 ± 7.5	92.6 ± 7.1	0.948

Data are the means plus/minus standard deviations. SBP, systolic blood pressure; DBP, diastolic blood pressure; MABP, mean arterial blood pressure; HC, healthy control; NA, not applicable.
* Pearson's chi-square test.

TABLE 2. Clinical Characteristics of Included Eyes

Variables	HC	NDON	DON	P
N	23	41	30	NA
BCVA, logMAR	−0.02 ± 0.06	0.08 ± 0.09	0.73 ± 0.50	<0.001
IOP, mm Hg	14.6 ± 2.7	17.6 ± 4.9	19.0 ± 4.7	0.002
Axial length, mm	23.6 ± 0.7	23.7 ± 0.9	23.2 ± 0.9	0.101
SE, diopter	0.1 ± 1.5	−0.5 ± 1.4	0.0 ± 1.6	0.245
VF-MD, dB	–	−4.20 ± 3.68	−14.03 ± 8.47	<0.001*
VF-PSD, dB	–	3.24 ± 1.75	7.27 ± 3.43	<0.001*
P100 latency, ms	–	106.4 ± 7.2	113.3 ± 15.1	0.013*
P100 amplitude, μV	–	12.20 ± 3.90	6.37 ± 3.88	<0.001*

Data are the means plus/minus standard deviations. IOP, intraocular pressure; SE, spherical equivalent.

* Data were obtained through independent samples t-test.

DISCUSSION

In the present study, we found that the vessel density in the peripapillary and macular areas significantly differs between TAO and healthy eyes. The onh-wiVD showed a desirable diagnostic accuracy to differentiate between DON and non-DON eyes. The rarefaction of peripapillary microvasculature, as surrogated by decreased onh-wiVD and rpc-wiVD, was positively correlated to the extent of visual impairment. To our best knowledge, this is the first study using OCT-A investigating the change of retinal vessel density in DON individuals.

The pathogenesis and mechanism underlying DON appears to be multifactorial, which might involve the optic nerve stretching by proptosis, elevated retrobulbar pressure, active intraorbital inflammation, and vascular insufficiency.[5] Previous studies have focused on the intraorbital blood flow in thyroid eye disease,[7,27] whereas little attention has been paid to intraocular hemodynamic changes, including retinal and choroidal circulation. In a recent study, retinal venous diameter in severe TAO eyes was found to be significantly decreased in comparison with controls,[28] and active TAO eyes had an increased retinal blood flow as measured by Heidelberg retina flowmeter.[29] In another case series of three patients, choroidal perfusion defects were noted in the eyes with the compressive optic neuropathy.[30] Interestingly, such defects were improved or completely resolved 1 year after orbital decompression surgery. Taken together, this evidence and the findings in our present study implied the retinal and choroidal perfusion might be associated with the onset and progression of DON.

With the emergence of OCT-A, the inspection of retinal microvasculature updated our understanding to the pathogenesis and mechanism of several critical eye diseases, such as glaucoma, ischemic optic neuropathy, and congenital ophthalmopathy.[31] Our findings of retinal microvascular attenuation in DON based on OCT-A implied that decreased microvascular perfusion was a progression accompanied by the development of TAO and was associated with impairment of visual functions.

Our findings somewhat contradict several previous reports. In a study investigating retinal blood flow by Heidelberg retina flowmeter in patients with TAO, increased retinal blood flow was found in active TAO patients compared to healthy controls. Consistently, Ye et al.[20] also found that active TAO patients presented with an increased retinal microvascular density. The discrepancy might mainly ascribe to the difference in study design: the participants these studies were primarily TAO patients uncomplicated with DON.

Rarefaction of the RPC in DON is another novel finding in our study. Reduced RPC density has been reported to be a major factor associated with the severity of several optic neuropathies. A similar relationship between RPC density reduction and visual impairment was also demonstrated in this study. The difference among the three groups might also suggest that RPC density was gradually decreased with the orbital compression becoming more serious. However, the ability of RPC density to distinguish DON from NDON patients is less desirable (AUROC, 0.65).

An intriguing finding was that both peripapillary and macular vessel density has been decreased in NDON patients versus healthy controls. It indicates that retinal vascular changes might precede functional changes, as represented by visual acuity and VF. The structural changes are common along with the progression,[32] and it has been reported that the peripapillary RNFL thickness was significantly thinner in chronic DON eyes compared to acute ones.[33] Combining the insignificant difference between healthy controls and NDON groups in structural parameters (i.e., RNFL and GCCL) in our study, we infer that a decrease in vessel density might be the earliest detectable change in the course of DON development. It would be an interesting topic to confirm the sequential damage of vessel structure function in DON in longitudinal studies.

TABLE 3. Macular Vessel Density in Healthy, Non-DON, and DON Eyes

Variables	HC	NDON	DON	P	Post Hoc Analysis P Values	
					NDON vs. HC	DON vs. NDON
m-wiVD	47.12 ± 2.52	44.27 ± 3.02	42.85 ± 3.39	<0.001	0.010	0.165
Fovea	26.18 ± 4.69	24.40 ± 4.66	25.45 ± 4.73	0.325	0.446	1.000
PF	49.10 ± 2.99	46.39 ± 3.35	45.16 ± 3.78	<0.001	0.009	0.408
Tempo	48.12 ± 3.23	46.04 ± 3.26	45.16 ± 3.20	0.005	0.045	0.793
Superior	50.10 ± 3.27	47.16 ± 3.79	42.28 ± 4.13	<0.001	0.010	0.199
Nasal	48.91 ± 2.92	46.21 ± 3.59	45.63 ± 3.96	0.003	0.014	1.000
Inferior	49.28 ± 3.73	46.15 ± 4.30	44.61 ± 5.13	0.001	0.025	0.458

Data are the means plus/minus standard deviations. PF, parafoveal.

TABLE 4. Optic Nerve Head Vessel Density in Healthy, Non-DON, and DON Eyes

| | | | | | Post Hoc Analysis *P* Values | |
Variables	HC	NDON	DON	*P*	NDON vs. HC	DON vs. NDON
onh-wiVD	56.70 ± 2.36	53.81 ± 3.27	50.26 ± 4.45	<0.001	0.006	<0.001
Inside-disc	53.62 ± 4.77	49.58 ± 5.31	46.42 ± 7.27	<0.001	0.03	0.085
Peripapillary	61.15 ± 3.57	58.70 ± 3.48	55.18 ± 5.31	<0.001	0.08	0.002
Nasal	58.51 ± 4.73	57.06 ± 4.17	54.55 ± 5.84	0.013	0.766	0.107
IN	61.08 ± 4.41	59.13 ± 4.92	56.86 ± 5.94	0.014	0.451	0.207
IT	65.67 ± 3.62	61.95 ± 5.49	57.63 ± 7.86	<0.001	0.059	0.011
ST	64.08 ± 3.32	61.61 ± 4.89	54.69 ± 5.91	<0.001	0.173	<0.001
SN	60.85 ± 4.74	58.3 ± 5.56	56.37 ± 5.49	0.013	0.213	0.410
Temporal	62.37 ± 4.34	57.74 ± 4.81	52.13 ± 6.47	<0.001	0.003	<0.001

Data are the means plus/minus standard deviations. IN, inferonasal; IT, inferotemporal; ST, supratemporal; SN, supranasal.

TABLE 5. Radial Peripapillary Capillary Density in Healthy, Non-DON, and DON Eyes

| | | | | | Post Hoc Analysis *P* Values | |
Variables	HC	NDON	DON	*P*	NDON vs. HC	DON vs. NDON
rpc-wiVD	54.73 ± 2.78	51.66 ± 3.75	48.90 ± 5.24	<0.001	0.011	0.014
Inside-disc	48.60 ± 7.06	42.45 ± 10.94	39.17 ± 8.96	0.002	0.045	0.464
Peripapillary	61.68 ± 3.71	58.73 ± 3.40	55.36 ± 5.40	<0.001	0.018	0.002
Nasal	57.14 ± 4.09	56.42 ± 3.86	53.51 ± 4.99	0.004	1.000	0.018
IN	61.28 ± 4.01	58.68 ± 5.32	57.61 ± 5.59	0.036	0.165	1.000
IT	67.44 ± 2.95	62.68 ± 5.48	58.64 ± 8.69	<0.001	0.013	0.027
ST	65.81 ± 3.91	62.64 ± 4.77	56.69 ± 5.86	<0.001	0.065	<0.001
SN	60.99 ± 4.56	57.94 ± 5.65	56.19 ± 5.24	0.006	0.086	0.517
Temporal	62.45 ± 4.01	58.54 ± 4.90	53.35 ± 5.44	<0.001	0.009	<0.001

Data are the means plus/minus standard deviations.

TABLE 6. RNFL and GCCL Thicknesses in Healthy, Non-DON, and DON Eyes

| | | | | | Post Hoc Analysis *P* Values | |
Variables	HC	NDON	DON	*P*	NDON vs. HC	DON vs. NDON
RNFL (μm)	104.91 ± 7.99	101.36 ± 8.64	98.30 ± 10.77	0.040	0.431	0.511
GCCL (μm)	100.30 ± 7.43	98.46 ± 14.53	90.52 ± 11.89	0.008	1.000	0.026

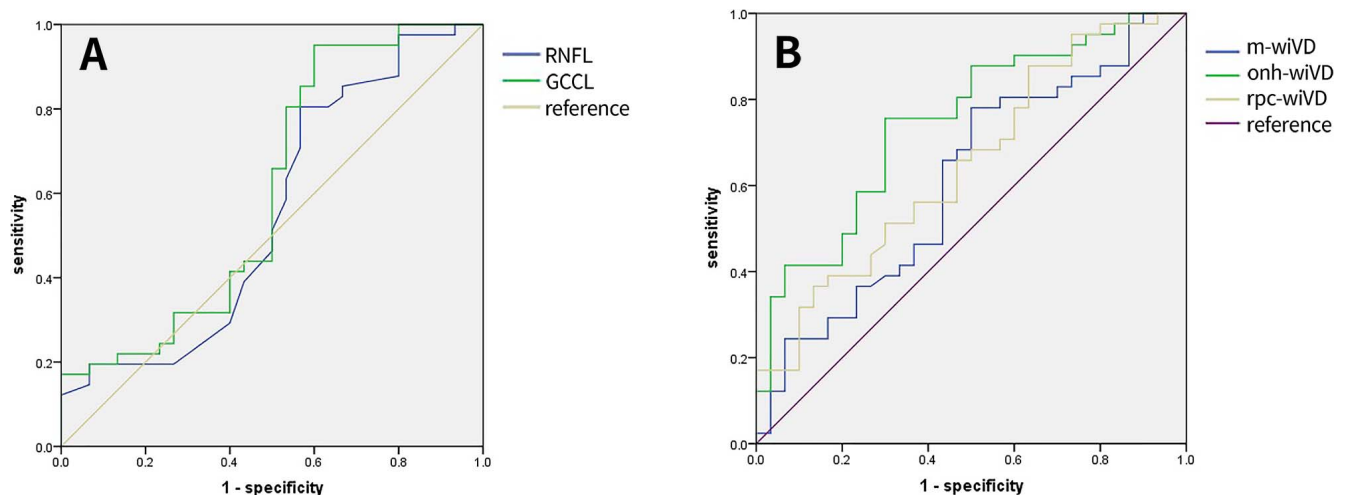Data are the means plus/minus standard deviations.

FIGURE 2. The area under the receiver operator characteristic curves (AUROCs) for differentiating DON from NDON eyes. (**A**) Retinal thickness measurements: GCCL thickness (0.61) and RNFL thickness (0.55), (**B**) retinal vessel densities: onh-wiVD (0.75), rpcwiVD (0.65), m-wiVD (0.61).

TABLE 7. Pearson Correlation Coefficient Matrix on Vessel Density Parameters and Visual Functions

Variables	RNFL	GCCL	m-wiVD	onh-wiVD	rpc-wiVD
BCVA (logMAR)	−0.302 (0.010)	−0.470 (<0.001)	−0.153 (0.202)	−0.507 (<0.001)	−0.424 (<0.001)
VF-MD	0.123 (0.308)	0.365 (0.002)	−0.024 (0.844)	0.264 (0.026)	0.272 (0.022)
VF-PSD	−0.097 (0.421)	−0.351 (0.003)	−0.044 (0.713)	−0.334 (0.004)	−0.324 (0.006)
P100 latency	−0.086 (0.474)	−0.286 (0.016)	−0.032 (0.789)	−0.336 (0.004)	−0.312 (0.008)
P100 amplitude	0.071 (0.555)	0.294 (0.013)	0.246 (0.039)	0.453 (<0.001)	0.408 (<0.001)

There are several limitations in the present study. First, there is no ideal method available to remove projection artifacts in OCT-A, so we only analyzed superficial retinal vessel density in the peripapillary and macular regions. Second, we did not take the disease course of DON (i.e., chronic or acute DON) into account. It has been reported that the peripapillary RNFL thickness was significantly thinner in chronic DON eyes compared to acute ones. It is unknown whether the DON staging would be associated with retinal vascular densities as well. Third, as a cross-sectional study, we are unable to figure out whether the microvascular alteration was the cause of functional damage in the neural retina or vice versa.

Our study showed the microvascular change among TAO patients and the correlations with structural parameters and visual function. On account of the results, we conclude the following: first, the m-wiVD changes early even when the visual function is not impaired; second, with the progress of the compression, the vessel density of ONH including rpc-wiVD and onh-wiVD decrease gradually; third, onh-wiVD has the sufficient ability to distinguish DON eyes from NDON eyes.

References

1. Wang Y, Smith TJ. Current concepts in the molecular pathogenesis of thyroid-associated ophthalmopathy. *Invest Ophthalmol Vis Sci*. 2014;55:1735–1748.

2. Dolman PJ. Grading severity and activity in thyroid eye disease. *Ophthalmic Plast Reconstr Surg*. 2018;34:S34–S40.

3. Bartley GB. The epidemiologic characteristics and clinical course of ophthalmopathy associated with autoimmune thyroid disease in Olmsted County, Minnesota. *Trans Am Ophthalmol Soc*. 1994;92:477–588.

4. Trobe JD, Glaser JS, Laflamme P. Dysthyroid optic neuropathy. Clinical profile and rationale for management. *J Arch Ophthalmol*. 1978;96:1199–1209.

5. Saeed P, Tavakoli Rad S, Bisschop P. Dysthyroid optic neuropathy. *Ophthalmic Plast Reconstr Surg*. 2018;34:S60–S67.

6. Blandford AD, Zhang D, Chundury RV, Perry JD. Dysthyroid optic neuropathy: update on pathogenesis, diagnosis, and management. *Expert Rev Ophthalmol*. 2017;12:111–121.

7. Konuk O, Onaran Z, Ozhan Oktar S, Yucel C, Unal M. Intraocular pressure and superior ophthalmic vein blood flow velocity in Graves' orbitopathy: relation with the clinical features. *Graefes Arch Clin Exp Ophthalmol*. 2009;247:1555–1559.

8. Potsaid B, Huang D, Subhash H, et al. Split-spectrum amplitude-decorrelation angiography with optical coherence tomography. 2012;20:4710–4725.

9. Tokayer J, Jia Y, Dhalla AH, Huang D. Blood flow velocity quantification using split-spectrum amplitude-decorrelation angiography with optical coherence tomography. *Biomed Opt Express*. 2013;4:1909–1924.

10. Shoji T, Zangwill LM, Akagi T, et al. Progressive macula vessel density loss in primary open-angle glaucoma: a longitudinal study. *Am J Ophthalmol*. 2017;182:107–117.

11. Triolo G, Rabiolo A, Shemonski ND, et al. Optical coherence tomography angiography macular and peripapillary vessel perfusion density in healthy subjects, glaucoma suspects, and glaucoma patients. *Invest Ophthalmol Vis Sci*. 2017;58:5713–5722.

12. Takusagawa HL, Liu L, Ma KN, et al. Projection-resolved optical coherence tomography angiography of macular retinal circulation in glaucoma. *Ophthalmology*. 2017;124:1589–1599.

13. Zhang S, Wu C, Liu L, et al. Optical coherence tomography angiography of the peripapillary retina in primary angle-closure glaucoma. *Am J Ophthalmol*. 2017;182:194–200.

14. Salz DA, de Carlo TE, Adhi M, et al. Select features of diabetic retinopathy on swept-source optical coherence tomographic angiography compared with fluorescein angiography and normal eyes. *JAMA Ophthalmol*. 2016;134:644–650.

15. Carlo TED, Filho MAB, Chin AT, et al. Spectral-domain optical coherence tomography angiography of choroidal neovascularization. 2015;122:1228–1238.

16. Ling JW, Yin X, Lu QY, Chen YY, Lu PR. Optical coherence tomography angiography of optic disc perfusion in nonarteritic anterior ischemic optic neuropathy. *Int J Ophthalmol*. 2017;10:1402–1406.

17. Liu CH, Wu WC, Sun MH, Kao LY, Lee YS, Chen HS. Comparison of the retinal microvascular density between open angle glaucoma and nonarteritic anterior ischemic optic neuropathy. *Invest Ophthalmol Vis Sci*. 2017;58:3350–3356.

18. Augstburger E, Zéboulon P, Keilani C, Baudouin C, Labbé A. Retinal and choroidal microvasculature in nonarteritic anterior ischemic optic neuropathy: an optical coherence tomography angiography study. *Invest Ophthalmol Vis Sci*. 2018;59:870–877.

19. Shin JW, Lee J, Kwon J, Choi J, Kook MS. Regional vascular density-visual field sensitivity relationship in glaucoma according to disease severity. *Br J Ophthalmol*. 2017;101:1666–1672.

20. Ye L, Zhou SS, Yang WL, et al. Retinal microvasculature alteration in active thyroid-associated ophthalmopathy. *Endocr Pract*. 2018;24:658–667.

21. Bartalena L, Baldeschi L, Dickinson AJ, et al. Consensus statement of the European group on Graves' orbitopathy (EUGOGO) on management of Graves' orbitopathy. *Thyroid*. 2008;18:333–346.

22. McKeag D, Lane C, Lazarus JH, et al. Clinical features of dysthyroid optic neuropathy: a European Group on Graves' Orbitopathy (EUGOGO) survey. *Br J Ophthalmol*. 2007;91:455–458.

23. Blandford AD, Zhang D, Chundury RV, Perry JD. Dysthyroid optic neuropathy: update on pathogenesis, diagnosis, and management. *Expert Rev Ophthalmol*. 2017;12:111–121.

24. Gao SS, Jia Y, Liu L, et al. Compensation for reflectance variation in vessel density quantification by optical coherence tomography angiography. *Invest Ophthalmol Vis Sci*. 2016; 57:4485–4492.

25. Jakimekjavic P, Beltram MJZV. Management of patients with graves' orbitopathy according to EUGOGO (European group on Graves' orbitopathy) consensus statement. *Zdrav Vestn Sup*. 2010;79:i34–i38.

26. Jia Y, Tan O, Tokayer J, et al. Split-spectrum amplitude-decorrelation angiography with optical coherence tomography. *Opt Express*. 2012;20:4710–4725.

27. Monteiro MLR, Moritz RBS, Angotti-Neto H, Benabou JE. Color Doppler imaging of the superior ophthalmic vein in patients with Graves' orbitopathy before and after treatment of congestive disease. *Clinics (Sao Paulo)*. 2011;66:1329–1333.

28. Yang X, Huang D, Ai S, Liang X, Zhao J, Fang L. Retinal vessel oxygen saturation and vessel diameter in inactive graves ophthalmopathy. *Ophthalmic Plast Reconstr Surg*. 2017;33: 459–465.

29. Perri P, Campa C, Costagliola C, Incorvaia C, D'Angelo S, Sebastiani A. Increased retinal blood flow in patients with active Graves' ophthalmopathy. *Curr Eye Res*. 2007;32:985–990.

30. Nik N, Fong A, Derdzakyan M, et al. Changes in choroidal perfusion after orbital decompression surgery for Graves' ophthalmopathy. *J Ophthalmic Vis Res*. 2017;12:183–186.

31. Cennamo G, Rossi C, Ruggiero P, De CG, Cennamo GJ. Study of the radial peripapillary capillary network in congenital optic disc anomalies with optical coherence tomography angiography. *Am J Ophthalmol*. 2017;176:1–8.

32. Sayin O, Yeter V, Ariturk N. Optic disc, macula, and retinal nerve fiber layer measurements obtained by OCT in thyroid-associated ophthalmopathy. *J Ophthalmol*. 2016;2016: 9452687.

33. Park KA, Kim YD, In Woo K, Kee C, Han JC. Optical coherence tomography measurements in compressive optic neuropathy associated with dysthyroid orbitopathy. *Graefes Arch Clin Exp Ophthalmol*. 2016;254:1617–1624.